Mathematical-Mechanical Model of WUF-B Connection Under Monotonic Load

HYUN CHANG YIM and TED KRAUTHAMMER

ABSTRACT

Connections in a steel frame are complex configurations composed of members and elements that contain different geometries, shapes and material properties. Therefore, one needs to take into account the contributions of such individual components to the overall connection behavior characteristics. This study presents a comprehensive mathematical-mechanical model to determine the welded unreinforced flange-bolted web (WUF-B) connection behavior. The model was developed considering nonlinear characteristics and coupling of individual component properties. The parameters in the mathematical expressions were derived based on collected data from numerical simulations, combined with modified and newly developed mechanical component equations. The models were evaluated by comparing them with finite element analysis results of nonlinear three-dimensional connections. The characterization models, (i.e., equations and procedures) introduced in this paper defined the mechanical properties of the WUF-B connections for a fast and accurate frame analysis of blast-oriented progressive collapse.

Keywords: welded unreinforced flange-bolted web connection, WUF-B, moment connections, mathematical modeling, finite element analysis.

Steel moment connections used in lateral load-resistant frames have shown a vulnerability to earthquakes, as observed in the Northridge earthquake (FEMA, 2000). The importance of beam to column connections was shown in progressive collapse studies (Krauthammer et al., 2004; Lim and Krauthammer, 2006). For relatively small local failures, strong connections enable the bridging of loads to undamaged structural columns. However, in the case of severe local damage by an abnormal load such as impact or blast, neighboring portions of the structure become unable to bridge the overloads and consecutive failures might be inevitable. Therefore, an accurate understanding of connection behavior is required for accurate progressive collapse analysis and to provide the necessary combination of ductility and strength in collapse-resistant frame design.

Considering the complexity of interactions between various parts in a connection, a finite element analysis (FEA) has been a viable approach for investigating such relationships. However, fully dynamic nonlinear FEA require significant computational resources. Analyzing even a single connection would require a sufficiently dense mesh for all components (including also bolts, nuts, welds, etc.), representation of contacts between the components, and representation of their fully nonlinear dynamic behaviors. Furthermore, numerical analyses of a three-dimensional multi-story building will require even more computational resources to derive and collect the structural behavior data. For instance, there are approximately 500 connections in a 10-story building with a plan layout of four bays by four bays. The numerical analyses of the whole structural system would be prohibitively long and expensive. Hence, it is essential to find a fast but reliable approach to characterize the detailed assemblies and to apply the properties for the joints of a frame model.

Moment-rotation ($M - \theta$) curves have been generally used to characterize steel connections and to provide the properties of connector elements of a building frame model. Although, $M - \theta$ curves can be derived either theoretically or numerically, such curves were typically created based on experimental test results. Cyclic tests were performed to determine the welded-unreinforced flange-bolted-web connections (WUF-B) properties (Krawinkler et al., 1971; Engelhardt et al., 1992, 1994). Krawinkler et al. (1971) suggested a trilinear model of the shear moment versus rotation behavior of the panel zone. Mathematical models were proposed using extensive test results (Nethercot, 1985; Kishi and Chen, 1986). Empirical models for several partially restrained connections were also introduced based on the experimental results, applying constant derivation techniques, such as curve fitting and regression analysis (Kishi, 1994; Attiogbe and Morris, 1991). Mathematical expressions for the connection properties were derived for computational frame analysis.

Hyun Chang Yim, Ph.D., Senior Researcher, Research Institute of Industrial Science and Technology (RIST), 79-5 Youngcheon, Dongtang, Hwaseong Gyeonggi-do 445-813 South Korea (corresponding author). E-mail: hcyim@rist.re.kr

Ted Krauthammer, Ph.D., Goldsby Professor of Civil Engineering and Director of the Center for Infrastructure Protection and Physical Security (CIPPS), Department of Civil and Coastal Engineering, University of Florida, 365 Weil Hall, Gainesville, FL 32611. E-mail: tedk@ufl.edu

Accurate representations of the moment-rotation relationships must be addressed, especially for the prediction of overall frame performance. One of the most often used equations for mathematical representations of force-deformation (or stress-strain) for a given structural connection system is the Richard-Abbott model (Richard and Abbott, 1975). Mechanical models are represented by component approaches proposed in Eurocode 3 (European Prestandard, 1997). These spring models were established with a set of components (spring elements) that contain inelastic constitutive properties quantified individually. The spring components are arranged in series or in parallel, and the assemblage can generate appropriate $M - \theta$ curves. The arrangement of springs, deformation contribution, and capacity of the weakest spring determine the initial rotational stiffness and flexural resistance capacity. The effectiveness of this method has been demonstrated by numerous studies (European Prestandard, 1995; Faella et al., 2000; Tamboli, 1999; Ivany and Baniotopoulos, 2000; Tschemmernegg, 1988; Simoes da Silva et al., 2002; Rassati et al., 2004). Some of these studies dealt with the direct flange-to-flange welded joints.

The present study is aimed at characterizing the WUF-B connection behavior via mathematical and mechanical representations. The characterization equations and procedures introduced in this paper define the mechanical properties of the WUF-B connections for a fast and accurate analysis of progressive collapse that could occur after abnormal loading such as blast. If the connection properties are only determined through experimental tests and FEA simulations with detailed and complex modeling, then it would require significant time and effort to investigate the entire frame collapse. Methods using mechanical components (springs) were employed to determine the connection properties, and the component equations were either newly developed in this study or adopted from a previous study and then modified. The equations were used to determine specific parameters in the mathematical model. Based upon the finite element analyses of a full three-dimensional connection model, the developed methods were evaluated for their ability to simplify the feasible configurations for fast-running algorithms used in structural assessment. Furthermore, the modified approach led to a much simplified input for such analyses that are quite feasible even in a design office environment.

MATHEMATICAL MODEL OF NONLINEAR MOMENT-ROTATION CURVE

Richard and Abbott (1975) proposed a mathematical representation for the nonlinear structural systems. The equation has been implemented for the determination of various load-response relationships such as stress-strain, force-deflection, and moment-curvature curves. Using the Richard-Abbott model, the moment-rotation relationship of a steel connection can be expressed, as follows (Richard and Abbott, 1975):

$$M = \frac{\left(K_e - K_p\right)\theta}{\left(1 + \left|\frac{K_e - K_p}{M_o}\right|^n\right)^{1/n}} + K_p\theta \tag{1}$$

where

K_e = rotational elastic stiffness
K_p = plastic stiffness
M_o = reference moment, and
n = shape factor.

The shape factor may be obtained by a two-point analytical expression on the curve, (θ_a, M_a), (θ_b, M_b). The value for n is given by Equation (2), as follows:

$$A^n - \frac{1}{2^n}\left(B^n - 1\right) = 0 \tag{2}$$

where

$A = \dfrac{K_i}{\left(K_a - K_p\right)}$

$B = \dfrac{K_i}{\left(K_b - K_p\right)}$

$K_a = M_a/\theta_a$

$K_b = M_b/\theta_b$

The shape factor, n is then determined by iterations. Therefore, in order to predict a moment-rotation property of an arbitrary connection, one should define four important parameters: elastic stiffness, plastic stiffness, a reference moment, and a shape factor.

CHARACTERIZATIONS OF THE WUF-B CONNECTIONS

Before identifying the parameters, we classified the WUF-B connections into two different types depending on their force transfers (Carter, 2003). In the first case, the total design moment is less than the flexural strength of the girder. This case is generally found in the designs for buildings located in wind and low-seismic zones. Continuity plates and doubler plates are seldom embedded in the column panel zone. The tensile and compressive forces from the girder's top and bottom flanges are transferred through the complete-joint-penetration groove welds into the column flanges and spread into the web. Shear forces are transmitted through a fillet-welded single plate (shear tab) on the girder web into the column web. The rotational behavior of this kind of connection is mostly formed inside the panel zone by the axial and shear deformations of the column web. In the second case—connections designed for high seismic applications—most of the rotation occurs at the end of the girder because the higher strength of the panel zone restrains the deformation.

Subsequently, this induces larger deformations into the weak girder end. The strength enhancement in the panel zone is achieved by selecting a larger size of column or using continuity plates and doubler plates. Such enhancement can shift the plastic hinge location into the girder end, even when the transferred moment is equal to the full flexural strength of the girder. Therefore, the rotation angle should be carefully defined based on the ratio of panel zone strength to girder strength. This study provides the proper definitions of the rotations for these cases and evaluates them by comparing the relationships of moment-connection rotation and moment-girder tip displacements between detailed and simplified numerical models.

The WUF-B connections can be categorized into the aforementioned two groups using the AISC design guideline for stiffening of wide-flange columns (Carter, 2003). In this study, either of two categories is used: a weak panel zone-strong girder (WPZ-SG), or a strong panel zone-weak girder (SPZ-WG). Compressive and tensile forces equivalent to the girder flexural limit moment are determined, as follows:

$$P_u = M_u / h_t \tag{3}$$

where

P_u = tensile or compressive axial force through girder top or bottom flange
M_u = girder flexural strength
h_t = moment arm length

Continuity plates are required if the obtained forces are greater than one of the following resisting strengths (AISC, 2005):

Column flange bending (tension force only),

$$\phi R_n = 0.9\left(6.25 t_{fc}^2 F_{yc}\right) \tag{4}$$

Column web yielding (tension and compression forces),

$$\phi R_n = 1.0\left(5k + t_{fg}\right) F_{yc} t_{wc} \tag{5}$$

Column web crippling (compression force only),

$$\phi R_n = 0.75\left(0.8\right) t_{wc}^{\ 2}\left[1 + 3\left(N/d_c\right)\left(t_{wc}/t_{fc}\right)^2\right] \times \sqrt{E\, F_{yc}\, t_{fc}\, / t_{wc}} \tag{6}$$

where

t_w = web thicknesses
t_f = flange thicknesses
d = depth of a member
F_y = yield strength
F_u = ultimate strength
E = modulus of elasticity
N = length of bearing
k = distance from outer face of flange to web toe of fillet weld

The subscripts c and g mean column and girder, respectively.

Meanwhile, a doubler plate is required if the transferred forces are greater than the column web shear strength, as follows:

$$\phi R_n = 0.9\left(0.6\right) F_{yc}\, d_c\, t_{wc} \text{ for } P_u = M_u / h_t < 0.4 F_{yc} A_c \tag{7}$$

$$\phi R_n = 0.9\left(0.6\right) F_{yc} d_c t_{wc}\left(1.4 - P_u / F_{yc} A_c\right) \text{ for } P_u = M_u / h_t \ge 0.4 F_{yc} A_c \tag{8}$$

The rotations of each group are defined, as illustrated in Figure 1. In the WPZ-SG connection, a rotating behavior is mostly observed in the panel zone, while the dominant

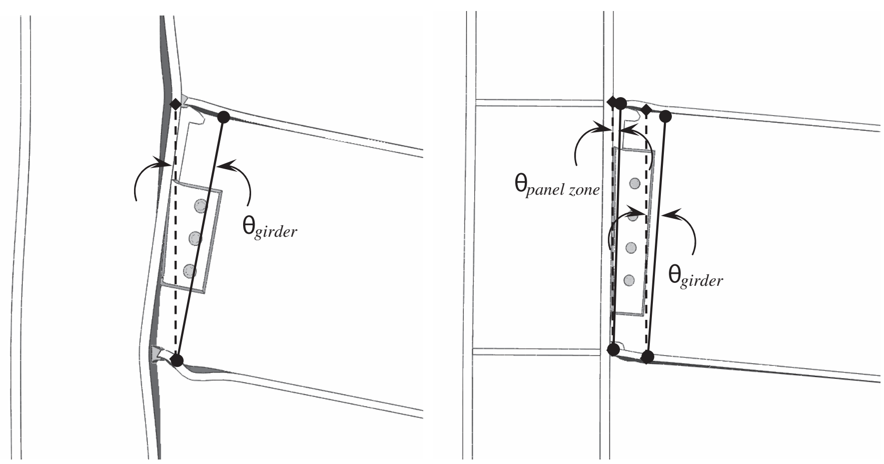

$\theta_{WPZ-SG} = \theta_{girder}$ $\theta_{SPZ-WG} = \theta_{girder} - \theta_{panel\ zone}$

(a) WPZ-SG connection *(b) SPZ-WG connection*

Fig. 1. Definition of rotations.

angle in the SPZ-WG connection is from the girder. This fact is shown by comparing moment-girder tip displacement relationships obtained from detailed and simplified models, as shown in Figures 2(a) and 2(b), respectively. First, a connection model was built as detailed as possible; i.e., considering full three-dimensional behaviors, bolt-nut pre-loading, contacts, and material and geometrical nonlinearity. These numerical studies used the finite element analysis program ABAQUS/Standard (Dassault Systems, 2008), and were validated in previous research (Yim and Krauthammer, 2009). Figure 3 indicate that the finite element models were successfully validated by comparison

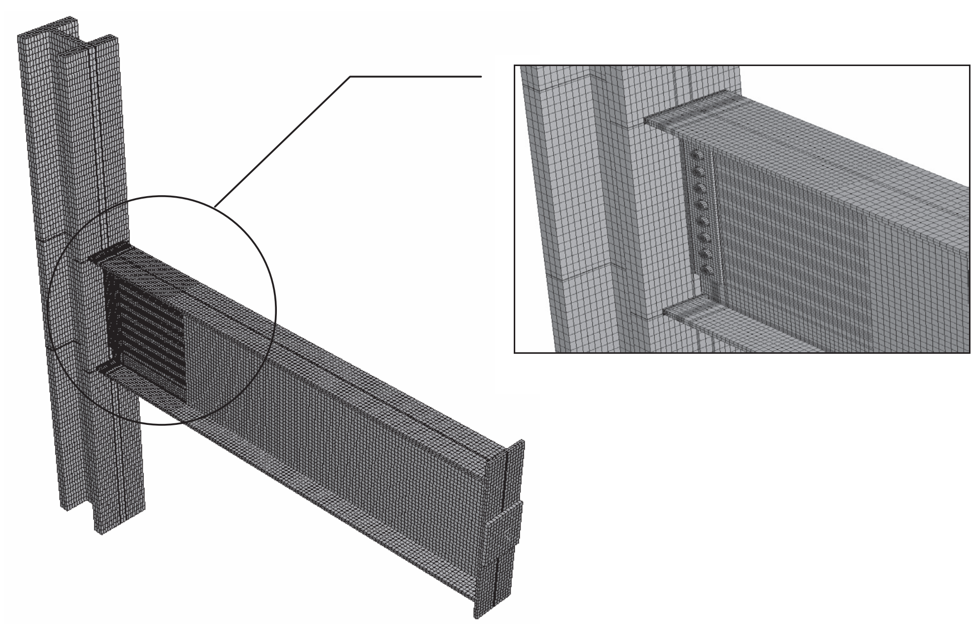

(a) Detailed model

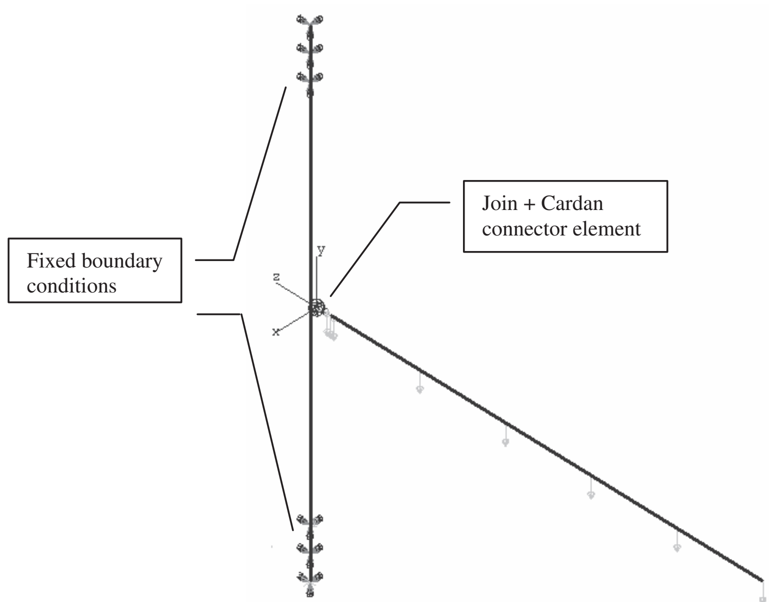

(b) Simplified model

Fig. 2. Detailed and simplified models.

with experimental data (Engelhardt and Sabol, 1994, for Case 16; Engelhardt and Husain, 1992, for Case 17 to Case 19; and Uang and Bondad, 1996, for Case 20). Based on the validated modeling techniques, push-down analyses where the static pressures were monotonically applied to the girders' top flange surfaces were conducted. The moment could be obtained by multiplying the applied pressures on the girder top flange by the lever arm lengths. The connection rotation was calculated from the displacements at the points close to the column flange and on the girder flanges (Figure 1), and the tip displacement was collected from the node of the girder tip in the neutral axis. Then, a finite element

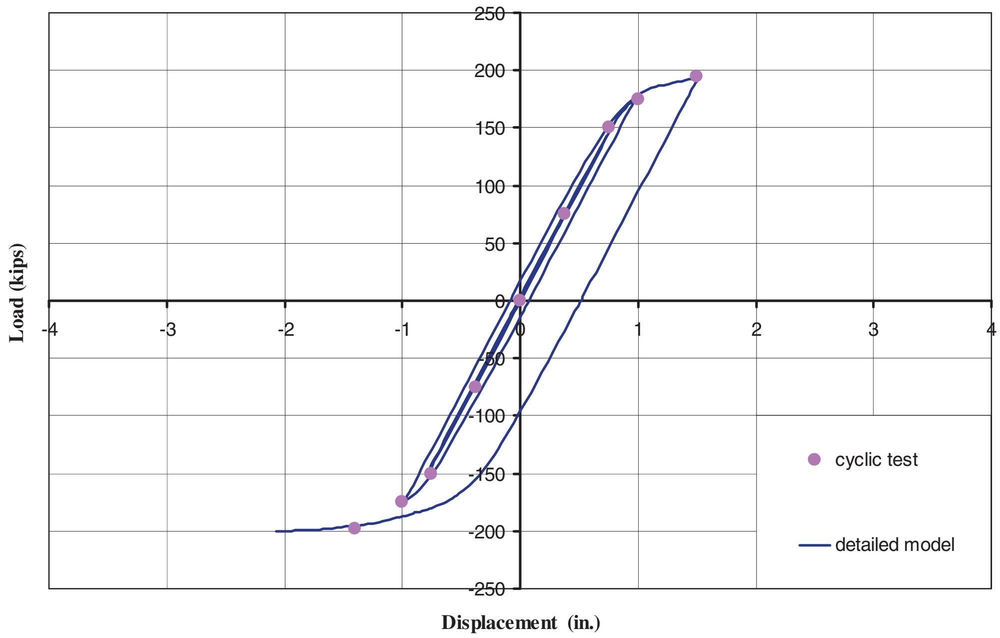

(a) Case 16 (Test result from Engelhardt and Sabol, 1994)

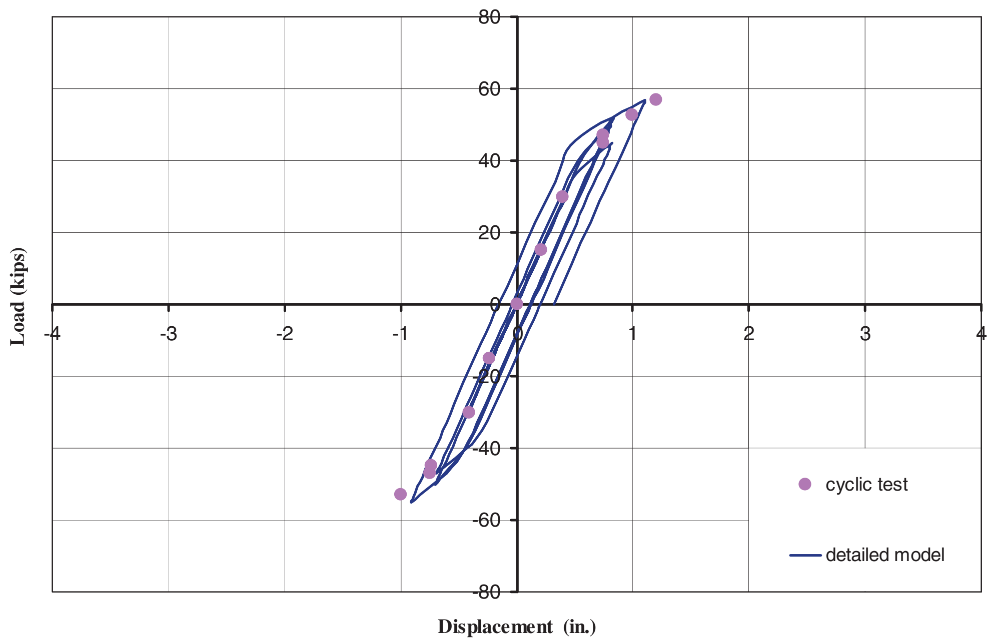

(b) Case 17 (Test result from Engelhardt and Husain, 1992)

Fig. 3. Result comparisons for model validation.

frame analysis was conducted with simpler beam elements and connector elements, as opposed to beam, column, and connection members modeled by 3D elements. All the same geometrical and material properties, boundary conditions, and loading, which had been adopted in the previous simulations for the detailed model, were applied into the simple frame analyses, as shown in Figure 2(b). The moment-rotation relationship extracted from the analysis with the detailed model was utilized as a mechanical property of the connector element in the simplified frame analyses.

Figures 4 and 5 are comparisons of moment-rotation ($M - \theta$) and moment-tip displacement ($M - \Delta$) relationships for detailed and simplified models. According to the comparisons, the simple models using the $M - \theta$ properties for both WPZ-SG and SPZ-WG connections proposed in this study could produce the $M - \Delta$ responses, which were in

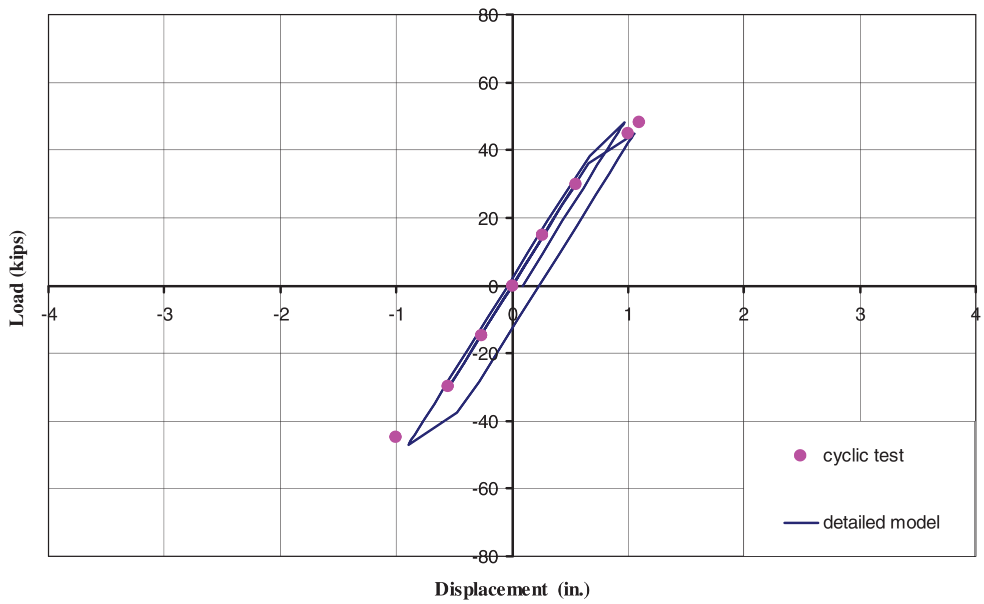

(c) Case 18 (Test result from Engelhardt and Husain, 1992)

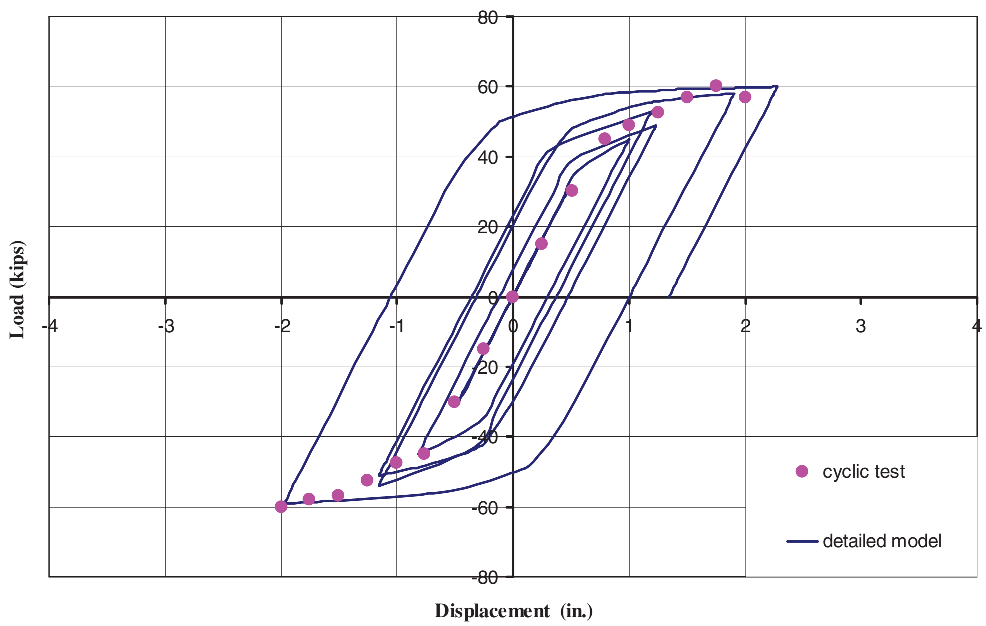

(d) Case 19 (Test result from Engelhardt and Husain, 1992)

Fig. 3. Result comparisons for model validation (continued).

Table 1. Number of Elements for Various Components (Case 16 in Table 3)		
Component	Number of Elements	
	Detailed Model	Simplified Model
Girder	21280	38
Column	39964	31
Bolts	6784	1 (Connector element)
Nuts	1024	
Shear Tabs	16680	
Welds	7158	
End Plate	176	

accord with the detailed model responses. Hence, it can be said that the rotations definition were accurate with respect to the specifically classified WUF-B connections.

In addition, it should be noted that the push-over simulations for the detailed models contained approximately 90,000 elements and required about 24 hours to run. The workstation had two Intel Xeon dual-core processors, operating at 3 GHz, and 3.5 GB of RAM for each CPU. The number of elements of individual members in the detailed and simplified models is defined in Table 1. The displacements from the simplified model were within 5 percent of the detailed model results and showed considerable savings in computation times and output file sizes (e.g., 12 hours run time and 1.20 GB of data, but less than 1 minute run time and 8 MB data for the simplified model). Hence, once the moment-rotation connection properties can be predicted mathematically and mechanically, the simplified models including these properties will be able to provide a good approximation of frame responses with very significant cost savings.

DERIVATION OF THE PARAMETERS IN THE MOMENT-ROTATION CURVES

In this study, the parameters of the mathematical representations were derived by means of a mechanical model, based on the Component Method (European Prestandard, 1997). In

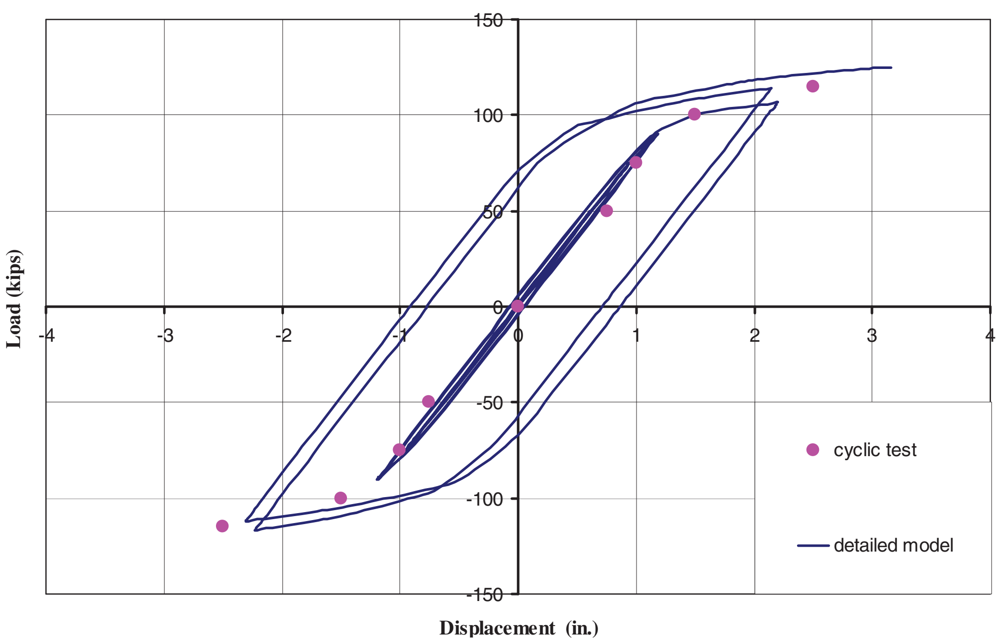

(e) Case 20 (Test result from Uang and Bondad, 1996)

Fig. 3. Result comparisons for model validation (continued).

particular, general approaches and terms presented in this study were adopted from previous research (e.g., Faella et al., 2000). One needs to modify the existing spring models or develop additional components (and those combinations), considering different force distributions in the unreinforced/reinforced panel zone to obtain more sophisticated $M - \theta$ curves.

The first step is the identification of the joint components. Seven basic components characterizing the WUF-B moment connection were considered (Figure 6): column web in shear (*cws*); column web in tension and compression (*cwt* and *cwc*); column flange in bending (*cfb*); girder flange in tension and compression (*gft* and *gfc*); and girder flange in tension/compression combined with shear tab in tension/compression (*gstab*).

As defined by Equation 1, the mathematical $M - \theta$ curve using the Richard-Abbott model is composed of the following four parameters: elastic and plastic stiffnesses, a reference moment, and a shape factor. The reference moment

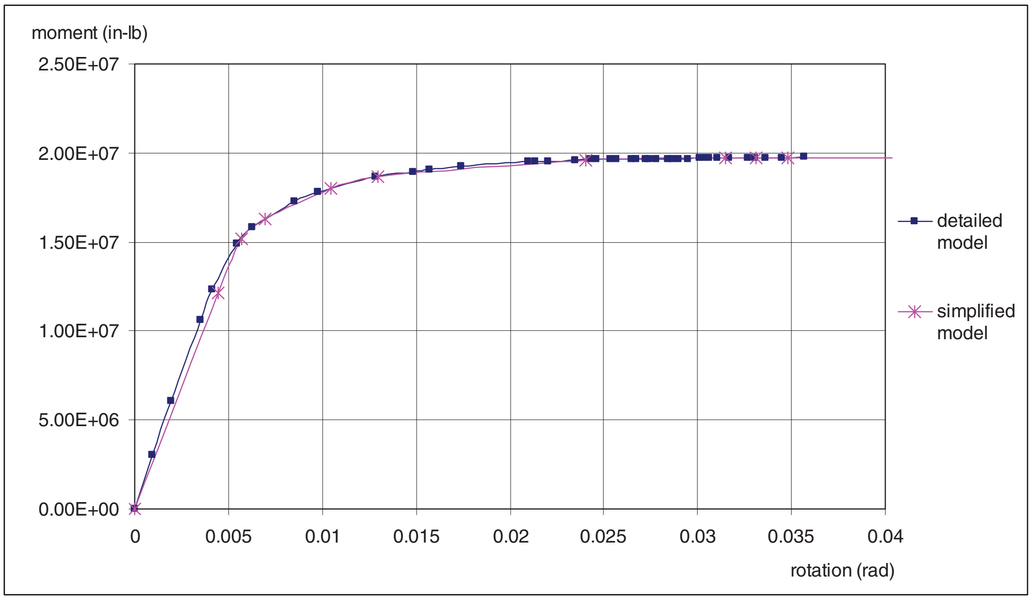

(a) Moment-rotation relationships

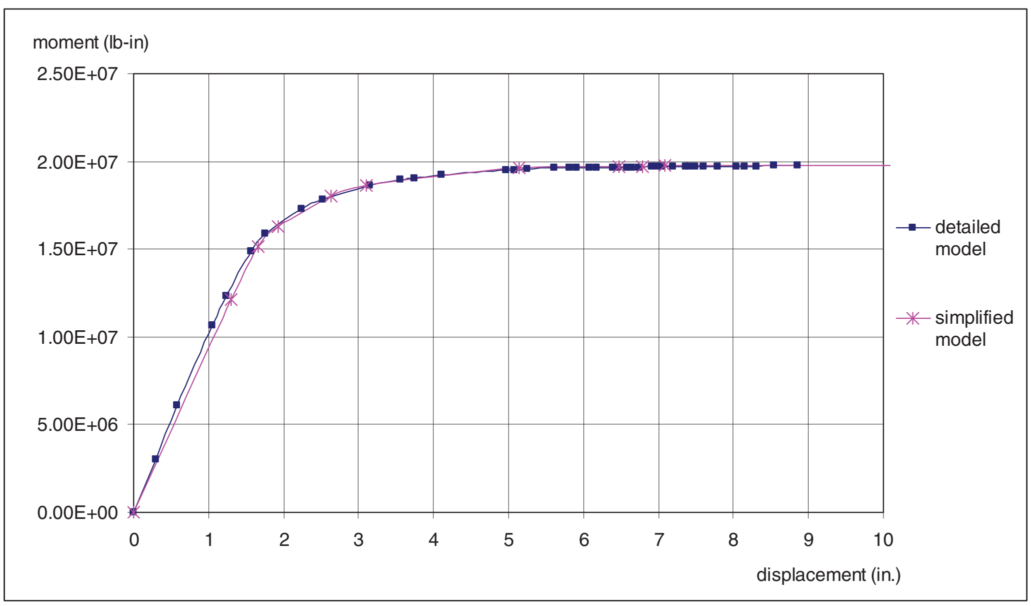

(b) Moment-tip displacement relationships

Fig. 4. WPZ-SG connection (Case 12 in Table 3).

and shape factor can be obtained using yield and ultimate moments. The governing components associated with each parameter are summarized in Table 2.

In the following sections, the component formulations and equation details are introduced in reference to each connection group. Procedures to extract the $M - \theta$ representations will then be presented. Finally, the reliability of the curve prediction will be discussed and demonstrated based on the comparisons with the simulation results.

Group 1: Weak Panel Zone-Strong Girder (WPZ-SG) WUF-B Connection

Elastic Stiffness

Components associated with the column web govern the elastic stiffness in this group. The stiffness component from the column web in shear can be obtained by the following fundamental moment-shear deformation relationship.

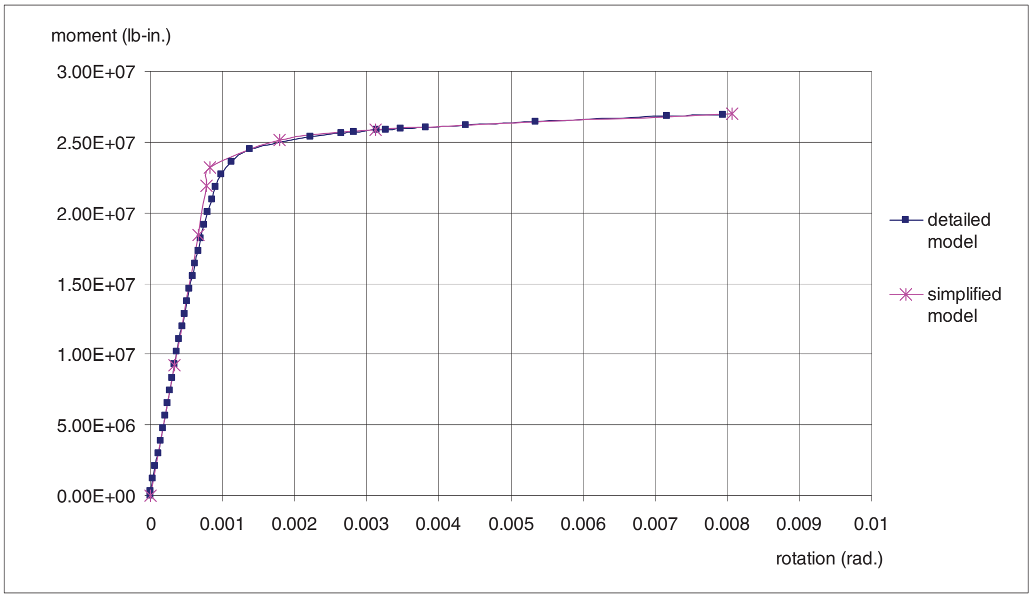

(a) Moment-rotation relationships

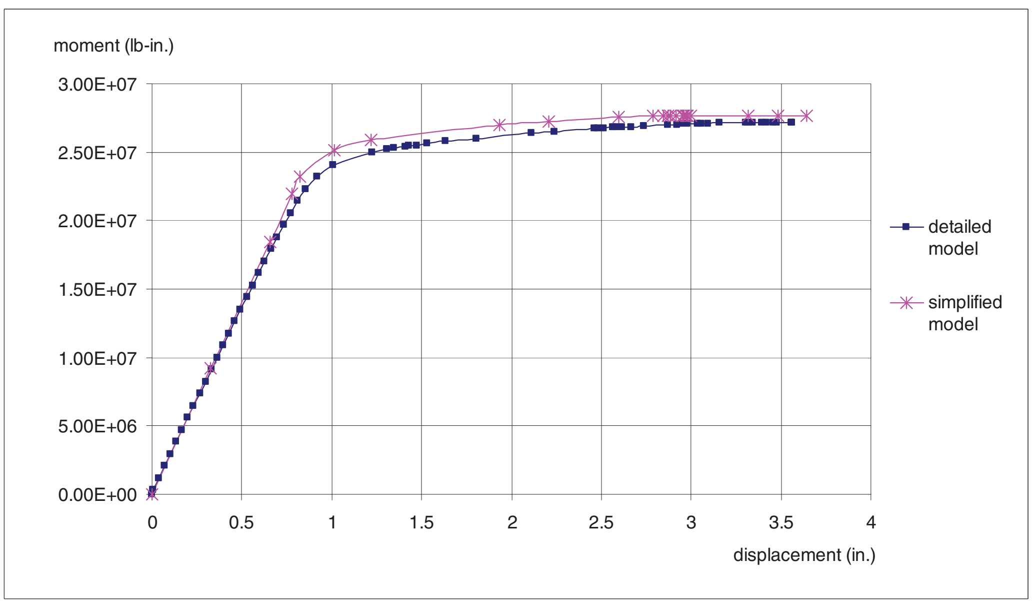

(b) Moment-tip displacement relationships

Fig. 5. SPZ-WG Connection (Case 16 in Table 3).

Table 2. Component List for the Related Parameters		
Parameters	**Components**	
	WPZ-SG connection	**SPZ-WG connection**
Elastic Stiffness	• column web in shear • column web in tension • column web in compression	• girder flange in tension • girder flange in compression
Yield Moment	• column web in shear • column web in tension • column web in compression • column flange in bending • girder flange in tension • girder flange in compression	• girder flange in tension • girder flange in compression
Plastic Stiffness	• girder web in tension • girder web in compression	• girder flange in tension • girder flange in compression
Ultimate Moment	• column web in tension or compression combined with shear tab force transfer • girder flange in tension/ compression, combined with shear tab in tension/ compression • groove weld failure	• girder flange in tension/ compression, combined with shear tab in tension/ compression • groove weld failure

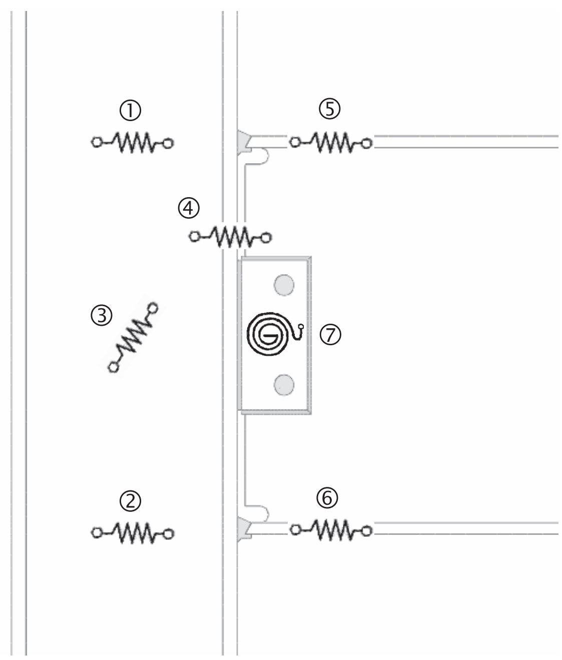

① column web in tension (*cwt*)

② column web in compression (*cwc*)

③ column web in shear (*cws*)

④ column flange in bending (*cfb*)

⑤ girder flange in tension (*gft*)

⑥ girder flange in compression (*gfc*)

⑦ shear tab in tension/compression (*gstab*)

Fig. 6. Components of WUF-B connection.

$$K_{cws} = \frac{GA_{vc}}{h_t} \tag{9}$$

The effective column web area is

$$A_{vc} = A_c - 2b_{fc}t_{fc} + \left(t_{wc} + 2r_c\right)t_{fc}$$

where

A_c = column area
r_c = radius of web-to-flange connection
G = shear modulus of elasticity

The stiffness characterized by the column web in tension and compression are identical, as shown in Equation 10,

$$K_{cwc} = K_{cwt} = \frac{Eb_{eff.cw}\,t_{wc}}{d_{wc}} \tag{10}$$

where

$b_{eff.\,cw}$ = effective width of the column web in tension and compression
d_{wc} = clear depth of the column web

The effective width $b_{eff.\,cw}$ is determined considering the action transmitted by the girder compressed flange, as shown in Equation 11 (European Prestandard, 1997):

$$b_{eff.cw} = t_{fg} + 2\sqrt{2}a_g + 5\left(t_{fc} + \sqrt{2}a_c\right) \tag{11}$$

where

t_{fg} = girder flange thickness
a_g = throat thicknesses of flange-to-web in girder
a_c = throat thicknesses of flange-to-web in column

One of the key features of the component method is the coupling of individual components. Since each component has an effect on the others during rotational behavior, a series formulation of the springs should be taken into account to define the constitutive model, as follows:

$$K_e = \frac{h_t^{\,2}}{\dfrac{1}{K_{cws}} + \dfrac{1}{K_{cwt}} + \dfrac{1}{K_{cwc}}} \tag{12}$$

Yield Moment

The flexural resistance can be determined from the weakest components, as expressed in Equation 13,

$$\begin{aligned} M_y &= F_{y\,\min}h_t \\ &= \min\left[F_{cws}, F_{cwc}, F_{cwt}, F_{cfb}, F_{gfc}, F_{gft}, F_{gfcb}\right]\cdot h_t \end{aligned} \tag{13}$$

First, the component strength in terms of column web in shear is given by Equation 14,

$$F_{cws} = \frac{f_{y\,pz}A_{vc}}{\sqrt{3}\,h_t\left(1 - h_t / L_c\right)} \tag{14}$$

where

$f_{y\,pz}$ = panel zone strength
L_c = column length

Next, the strength of the column web in compression is the minimum value of crushing or buckling resistance, as shown in Equation 15,

$$F_{cwc} = \min\left[F_{cwc\ crushing}, F_{cwc\ buckling}\right] \tag{15-1}$$

$$F_{cwc\ crushing} = b_{eff.cw}t_{wc}f_{y.cw} \tag{15-2}$$

The buckling resistance was determined by the use of the classical Winter formula (Faella et al., 2000). If the slenderness $\bar{\lambda} = \left(\dfrac{b_{eff.cw}t_{wc}f_{y.cw}}{F_{cr}}\right)^{1/2}$ is greater than 0.67, where

$F_{cr} = \dfrac{\pi E t_{wc}^{\ 3}}{3\left(1 - v^2\right)d_{wc}}$, then

$$F_{cwc\ buckling} = b^{*}_{eff.cwc}t_{wc}f_{y.cw}\frac{1}{\bar{\lambda}}\left(1 - \frac{0.22}{\bar{\lambda}}\right) \tag{15-3}$$

where

$$b^{*}_{eff.cwc} = t_{fb} + 2\left(t_{fc} + r_c\right)\left[\bar{\psi}\left(\frac{d_{wc}b_{fc}}{3t_{wc}t_{fc}}\right)^{1/4}\right]$$

= effective width for buckling resistance
$\bar{\psi}$ = reduction coefficient on the actual restraining action from column web

If $\bar{\lambda}$ is less than 0.67, $F_{cwc\ buckling} = F_{cwc\ crushing}$.

Equation 16 provides the load carrying capacity of the column web in tension,

$$F_{cwt} = b_{eff.cw}t_{wc}f_{y.cw} \tag{16}$$

Equation 17 can be used for flexural strength by means of a column flange in bending.

$$F_{cwc} = b_{eff.cfb}t_{fg}f_{y.gf} + \frac{t_{wg}d_{wg}f_{y.gw}}{4\left(h_g - t_{fg}\right)} \tag{17}$$

where

d_{wg} = clear depth of girder web
$f_{y\,gw}$ = yield strengths of girder web
$f_{y\,gf}$ = yield strengths of girder flange
$b_{eff.cfb} = t_{wc} + 2r_c + 7kt_{fc}$
= effective width for column flange bending
$k = \dfrac{f_{y.cf}t_{fc}}{f_{y.gf}t_{fg}}$ = coefficient

If the panel zone is relatively stronger than a portion of the girder, plastic behavior of connection initiates at the groove-welded girder flanges. Therefore, the resistance capacity of the girder flange is given by the following:

$$F_{gft} = F_{gfc} = \min\left[f_{cr\ gf}, f_{y\ gf}\right]b_{fg}t_{fg} \tag{18}$$

The $f_{cr\,gf}$ is the flange strength to resist local buckling defined as (AISC, 2005):

$$f_{cr\,gf} = \frac{k\pi^2 E}{12\left(1-\mu^2\right)\left[\frac{\left(b_{fg}/2\right)}{t_{fg}}\right]^2} \geq f_{y\,gf} \tag{19}$$

where
- μ = Poisson's ratio
- k = constant depending on plate conditions (0.7 for flange)

Plastic Stiffness

Once yielding occurs in the panel zone before the girder end reach fully plastic condition, the girder flanges will contribute to the rotational plastic hardening behavior. Therefore,

$$K_{gft} = K_{gfc} = \frac{Eb_{fg}t_{fg}}{\rho b_{stab}} \tag{20}$$

where
- ρ = coefficient
- b_{stab} = width of shear tab plate

If the panel zone reaches the ultimate condition, ρ is 1.0. When the ultimate stress is found at the girder flange zone, ρ is 1.5. Considering the series of springs and material hardening ratio, $\frac{E_h}{E}$, the plastic stiffness can be computed by Equation 21:

$$K_p = \frac{E_h}{E}\left(K_{eg}\right) = \frac{E_h}{E}\left(\frac{h_t^2}{\frac{1}{K_{gft}}+\frac{1}{K_{gfc}}}\right) \tag{21}$$

Ultimate Moment

Ultimate flexural resistance can be obtained from the weakest component ultimate strength as expressed in Equation 22:

$$M_u = F_{u\,\min} h_t = \min\left[F_{cw\,stab}, F_{g\,stab}, F_{gweld}\right] h_t \tag{22}$$

where
- $F_{cw\,stab}$ = force by the column web in compression or tension, adding the forces transferred through shear tab
- $F_{g\,stab}$ = force from the girder in tension/compression combined with shear tab force
- F_{gweld} = force by ultimate strength of groove weld between girder and column

The specific expressions are shown in Equations 23 and 24, respectively:

$$F_{cw\,stab} = t_{wc} f_{u.cw}\left[b_{eff.cwc} + \left(h_{stab}/2\right)^2\right] \tag{23}$$

$$F_{g\,stab} = \left[f_{y\,gf} + \frac{\left(f_{u\,gf} - f_{y\,gf}\right)}{3}\right] b_{fc} t_{fc} h_t + \left[f_{u\,stab}\; t_{stab}\left(\frac{h_{stab}}{2}\right)^2 - \left(f_{u\,stab} - f_{y\,stab}\right) t_{stab}\left(\frac{h_{stab}^2}{8}\right)\right] \tag{24}$$

where
- h_{stab} = height of shear tab plate
- t_{stab} = thickness of shear tab plate

Also,

$$F_{gweld} = f_{u\,gweld} b_{fg}\, t_{fg} \tag{25}$$

where $f_{u\,gweld}$ is the ultimate strength of groove weld.

It should be noted that the ultimate moment is produced by means of interactions between the panel zone and the girder. In particular, it will be more complicated if the panel zone yields before the girder and the shear tab plate reaches its ultimate conditions. Therefore, in the WPZ-SG case, the ultimate and yield forces are assumed to be distributed in the shape of concave and convex ellipses on the cross sections on shear tab plates and girder flanges, respectively, as shown in Figure 7.

Strong Panel Zone-Weak Girder (SPZ-WG) WUF-B Connection

Elastic Stiffness

As a panel zone is made stronger by increasing column size or reinforcing, the rotation behavior becomes more concentrated at the girder region. Therefore, the stiffness is obtained on the basis of girder flanges in tension and compression, similar to the plastic hardening stiffness of a WPZ-SG connection. The initial stiffness is given by:

$$K_e = K_{eg} = \frac{h_t^2}{\frac{1}{K_{gft}}+\frac{1}{K_{gfc}}} \tag{26}$$

where K_{gft} (equal to K_{gfc}) is the girder flange stiffness introduced in Equation 20. Because the ultimate stress occurs at the girder flange zone, ρ is assumed to be 1.5.

Yield Moment

Since the girder flange zone is weaker than the panel zone, the yield resistance of an SPZ-WG connection can be computed by Equation 18.

Plastic Stiffness

The plastic stiffness of an SPZ-WG case is identical to the WPZ-SG connection, where the ultimate stress is found in the girder flanges (Equation 21).

Ultimate Moment

The ultimate moment of an SPZ-WG connection can be obtained using the approach for a WPZ-SG connection, and the ultimate strength is found in the girder zone, as represented by Equation 24. As shown in Equation 27, the only difference is that the full ultimate stress was applied instead of the elliptical stress distribution. This is because one expects more contribution from the girder region in the case of the strong-panel zone connection.

$$F_{g\ stab} = f_{u\ gf} b_{fc} t_{fc} h_t + \left[f_{u\ stab}\ t_{stab} \left(\frac{h_{stab}}{2} \right)^2 - \left(f_{u\ stab} - f_{y\ stab} \right) t_{stab} \left(\frac{h_{stab}^{\ 2}}{8} \right) \right] \tag{27}$$

COMPARISONS WITH SIMULATION RESULTS

To show the accuracy of the mathematical-mechanical models, this study included extensive comparisons of the $M - \theta$ curves computed by the aforementioned approach with numerical analysis conducted by ABAQUS/Standard (Dassault Systems, 2008). Various girder-column candidates were employed or designed, as summarized in Table 3. For the WPZ-SG and WUF-B connections (from Cases 1 through 12), girder-column combinations and connections were employed from a building assumed to be located in a low-seismic zone, and the connections were designed on the basis of the pre-Northridge design concept. For the SPZ-WG cases, three connections were designed based on the AISC *Manual* (AISC, 2005). The column panel zones were reinforced by continuity plates and doubler plates. Cases 16 to 20 were obtained from seismic test studies (Engelhardt and Husain, 1992; Engelhardt and Sabol, 1994; and Uang and Bondad, 1996). These eight SPZ-WG connections were designed to have highly stiff panel zones compared to the flexural strength of the joined girders.

The finite element models were established using ABAQUS/Standard, as shown in Figure 2. An elasto-plastic material property with isotropic hardening was selected to simulate the material behavior of all the components of the finite element model. The material models are shown in Table 4. An elastic modulus of 29,000 ksi, Poisson's ratio of 0.3, and ultimate strain of 0.2 were used for all cases. It should be noted that the girder and column properties of Cases 16 to 20 followed the mill certificate strength data reported on the experimental study (Engelhardt and Husain, 1992; Engelhardt and Sabol, 1994; and Uang and Bondad, 1996) while those of Cases 1 to 15 were constructed with ASTM A992 steel. Shear tabs of ASTM A36 steel, A325N bolts, and E70T-7 welds were used for all cases. The element types mainly used for the finite element models in this study were eight-node continuum (brick) elements with reduced integration (C3D8R). Six-node wedge elements (C3D6) were also used to model the curved parts that included the weld access holes, bolt holes and welds (Dassault Systems, 2008).

The numerical simulation results were compared with the results predicted by the proposed models. In Cases 1 through 4, the mechanical model results showed that both initial yield and ultimate moments were found in the panel zones, since the zones were weaker than girder region. Next, in Cases 5 to 8, it was shown that the yield moment occurs in the panel zones first, but the ultimate moment occurs at the girders. In Cases 9 to 12, both yield and ultimate moments were obtained from the girder regions, even though some portion of the panel zones yielded. Meanwhile, as expected before, the rotations were governed by girder deformations

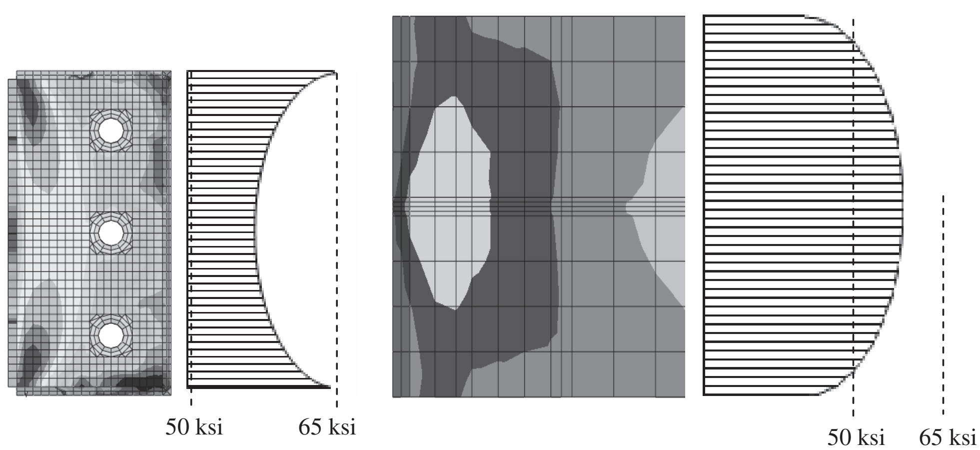

(a) Shear tab (elevation view) *(b) Girder flange (top view)*

Fig. 7. Stress distributions on the shear tab and girder flange cross sections.

Table 3. Connection Cases

	No.	Girder	Column	Shear Tab Plate					Bolt			Weld		Continuity Plate			Doubler Plate	
				b_{stab}	h_{stab}	t_{stab}	L_{ev}	L_{eh}	ϕ	N_b	s	$t_{w\ stab\text{-}cflange}$	$t_{w\ stab\text{-}gweb}$	b_{stiff}	w_{stiff}	t_{stiff}	t_{dp}	2–t_{dp}
WPZ-SG	1	W21×62	W14×74	4½	9	5/16	1.5	1.5	¾	3	3	5/16	3/16	0	0	0	0	0
	2	W21×57	W14×99	4½	9	5/16	1.5	1.5	¾	3	3	5/16	3/16	0	0	0	0	0
	3	W27×94	W14×90	4½	15	5/16	1.5	1.5	¾	4	4	5/16	3/16	0	0	0	0	0
	4	W30×99	W14×90	4½	15	¼	1.5	1.5	¾	4	4	¼	¼	0	0	0	0	0
	5	W24×76	W14×120	4½	9	5/16	1.5	1.5	¾	3	3	5/16	3/16	0	0	0	0	0
	6	W27×94	W14×176	4½	15	5/16	1.5	1.5	¾	4	4	5/16	3/16	0	0	0	0	0
	7	W30×108	W14×132	4½	15	5/16	1.5	1.5	¾	4	4	5/16	¼	0	0	0	0	0
	8	W30×116	W14×159	4½	15	5/16	1.5	1.5	¾	4	4	5/16	¼	0	0	0	0	0
	9	W18×35	W14×74	4½	9	5/16	1.5	1.5	¾	3	3	5/16	3/16	0	0	0	0	0
	10	W18×35	W14×99	4½	9	5/16	1.5	1.5	¾	3	3	5/16	3/16	0	0	0	0	0
	11	W30×116	W14×233	4½	15	5/16	1.5	1.5	¾	4	4	5/16	¼	0	0	0	0	0
	12	W36×135	W14×283	4½	19	⅜	1.5	1.5	1	5	4	5/16	¼	0	0	0	0	0
SPZ-WG	13	W21×44	W12×53	3	12	¼	3	1.5	⅝	3	3	¼	3/16	4 3/16	11	7/16	1	½
	14	W24×62	W14×120	3	15	¼	3	1.5	⅝	4	3	5/16	3/16	7	12⅝	9/16	1	½
	15	W24×68	W12×252	3	15	5/16	3	1.5	¾	4	3	5/16	¼	0	0	0	1	½
	16	W36×150	W14×455	5	25	⅝	1.5	1.5	1	8	3	5/16	¼	0	0	0	0	0
	17	W24×55	W12×136	4½	18	½	1.5	1.5	⅞	6	3	5/16	0	5¾	10⅞	½	0	0
	18	W18×60	W12×136	4½	12	½	1.5	1.5	⅞	4	3	5/16	0	5¾	10⅞	½	0	0
	19	W21×57	W12×136	4½	15	½	1.5	1.5	⅞	5	3	5/16	0	5¾	10⅞	½	0	0
	20	W30×99	W14×176	4½	24	⅝	1.5	1.5	⅞	8	3	5/16	5/16	7 7/16	12 9/16	⅜	0	0

b_{stab} = width of shear tab plate (in.)
h_{stab} = height of shear tab plate (in.)
t_{stab} = thickness of shear tab plate (in.)
L_{ev} = vertical length from edge to first bolt hole (in.)
L_{eh} = horizontal length from edge to first bolt hole (in.)
ϕ = bolt diameter (in.)
N_b = number of bolts
s = bolt spacing (in.)
$t_{w\ stab\text{-}cflange}$ = thickness of weld between shear tab plate and column flange (in.)
$t_{w\ stab\text{-}gweb}$ = thickness of weld between shear tab plate and girder web (in.)
b_{stiff} = length of continuity plate (in.)
w_{stiff} = width of continuity plate (in.)
t_{stiff} = thickness of continuity plate (in.)
t_{dp} = thickness of doubler plate (in.)

in the SPZ-WG connections (Cases 13 to 16). Table 5 summarizes the overall results from simulations and mechanical representations.

Once the yield or ultimate moments and elastic or plastic stiffnesses are computed, the next step was to generate the parameters for the mathematical representations (Equation 1). The required parameters, θ_a, M_a, θ_b, M_b, M_o and n are defined by Equations 28-1 through 28-5. The shape factor n is then determined through iteration, as defined by Equation 2.

$$M_a = M_y \tag{28-1}$$

$$\theta_a = \theta_y = M_y / K_e \tag{28-2}$$

$$M_0 = M_y + \frac{\eta}{3}\left(M_u - M_y\right) \tag{28-3}$$

$$\theta_b = 2\theta_a \tag{28-4}$$

$$M_b = M_y + \left(M_u - M_y\right)\left(\frac{\theta_b - \theta_a}{\theta_u - \theta_y}\right) \tag{28-5}$$

where $\eta = 1$ if the beam web supplemental weld is not provided and $\eta = 2$ if such a weld is provided.

Table 4. Connection Component Yield and Ultimate Strengths						
Case	Strength	Girder	Column	Shear Tabs	Bolt/Nut	Weld
1-15	f_y (ksi)	50.0/50.0	50.0/50.0	36.0	92.0	70.0
	f_u (ksi)	65.0/65.0	65.0/65.0	58.0	120.0	80.0
16[a]	f_y (ksi)	50.0/50.0	62.5/62.5	50.0	92.0	70.0
	f_u (ksi)	64.8/64.8	78.9/78.9	64.8	120.0	80.0
17[b]	f_y (ksi)	41.6/42.3	52.0/54.9	36.0	92.0	58.0
	f_u (ksi)	59.6/63.9	70.4/73.7	58.0	120.0	70.0
18[b]	f_y (ksi)	40.9/43.0	52.0/54.9	36.0	92.0	58.0
	f_u (ksi)	59.9/59.9	70.4/73.7	58.0	120.0	70.0
19[b]	f_y (ksi)	38.4/36.5	52.0/54.9	36.0	92.0	58.0
	f_u (ksi)	56.1/54.7	70.4/73.7	58.0	120.0	70.0
20[c]	f_y (ksi)	46.5/57.1	52.5/51.2	36.0	92.0	58.0
	f_u (ksi)	67.7/72.5	68.2/67.2	58.0	120.0	70.0

[a] Engelhardt and Sabol, 1994
[b] Engelhardt and Husain, 1992
[c] Uang and Bondad, 1996

Table 5. Results from Mathematical-Mechanical Models and Simulations									
	No.	K_e (in.-lb-rad)		M_y (in.-lb)		K_p (in.-lb-rad)		M_u (in.-lb)	
		Simulation	Math.-Mech.	Simulation	Math.-Mech.	Simulation	Math.-Mech.	Simulation	Math.-Mech.
WPZ-SG	1	5.92E+08	6.71E+08	3.34E+06	2.57E+06	1.50E+07	1.85E+07	4.78E+06	5.08E+06
	2	7.40E+08	7.23E+08	3.32E+06	2.96E+06	1.30E+07	1.57E+07	5.46E+06	5.18E+06
	3	2.76E+10	2.67E+10	4.81E+06	3.29E+06	4.56E+07	4.48E+07	6.85E+06	6.36E+06
	4	1.04E+09	1.09E+09	5.05E+06	3.60E+06	4.58E+07	5.22E+07	7.61E+06	7.47E+06
	5	1.10E+09	1.14E+09	3.64E+06	4.65E+06	3.06E+07	1.94E+07	7.82E+06	8.11E+06
	6	1.68E+09	2.12E+09	9.36E+06	9.45E+06	3.25E+07	2.99E+07	1.22E+07	1.12E+07
	7	1.67E+09	1.79E+09	6.38E+06	6.86E+06	4.33E+07	3.95E+07	1.27E+07	1.36E+07
	8	1.91E+09	2.15E+09	8.50E+06	8.92E+06	5.49E+07	4.45E+07	1.56E+07	1.51E+07
	9	4.78E+08	5.10E+08	2.13E+06	2.13E+06	5.66E+06	4.46E+06	2.82E+06	2.76E+06
	10	5.27E+08	5.46E+08	2.13E+06	2.20E+06	5.06E+06	4.46E+06	2.82E+06	2.76E+06
	11	2.54E+09	3.49E+09	1.26E+07	1.30E+07	3.43E+07	4.45E+07	1.55E+07	1.51E+07
	12	3.84E+09	5.58E+09	1.63E+07	1.65E+07	5.54E+07	6.74E+07	1.97E+07	1.95E+07
SPZ-WG	13	5.36E+09	5.80E+09	3.55E+06	2.96E+06	1.06E+07	1.58E+07	3.97E+06	4.27E+06
	14	9.10E+09	1.07E+10	5.16E+06	4.80E+06	2.26E+07	2.93E+07	5.94E+06	6.90E+06
	15	1.21E+10	1.36E+10	6.99E+06	6.06E+06	4.43E+07	3.70E+07	8.27E+06	8.71E+06
	16	2.76E+10	2.67E+10	2.32E+07	1.97E+07	1.38E+08	1.09E+08	2.94E+07	3.12E+07
	17	5.98E+09	4.06E+09	3.42E+06	2.94E+06	1.05E+08	1.01E+08	5.64E+07	5.85E+06
	18	4.36E+09	3.46E+09	3.42E+06	3.31E+06	9.34E+07	9.93E+07	5.69E+06	5.44E+06
	19	3.90E+09	3.83E+09	3.71E+06	3.14E+06	1.14E+08	9.88E+07	5.91E+06	6.12E+06
	20	1.41E+09	1.27E+10	1.19E+07	8.91E+06	1.20E+08	9.37E+07	1.50E+07	1.67E+07

Finally, the $M - \theta$ curves are derived and compared with the curves extracted from the simulations. The comparisons in Figures 8 demonstrate that the theoretical curves were in quite good agreement with those from the finite element analyses.

DISCUSSION

The Richard-Abbott model could be used to describe a nonlinear behavioral model for a moment connection using mechanical parameters and a shape factor. The strong point of the model is that it produces the nonlinear curves if points are defined before and after the point of inflection (i.e., before the curve between proportional limit and strain hardening). The points before the inflection were accurately determined by the initial stiffness and yield strength formulations given in this study. The connection yielding started at the panel zones in Cases 1 through 8 while the girder regions yielded first in Cases 9 to 20, due to the relatively stronger panel zones that moved the yield initiations into the girder regions. The simulation results for Cases 5 to 8 showed that the yielding initiated in the panel zones, but the girders reached the ultimate conditions earlier. This can happen because the panel zones are the stiffened regions, and they may resist the loads until the unstiffened girder flanges reached ultimate stresses. Stress concentrations around the weld access holes caused the ultimate moment condition at the girder to be reached sooner. In Cases 9 to 12, both yield and ultimate moments were obtained in the girder regions, even though some portion of the panel zones yielded. Meanwhile, as expected, the rotations were governed by girder deformations for the SPZ-WG connections (Cases 13 to 20). The differences in results

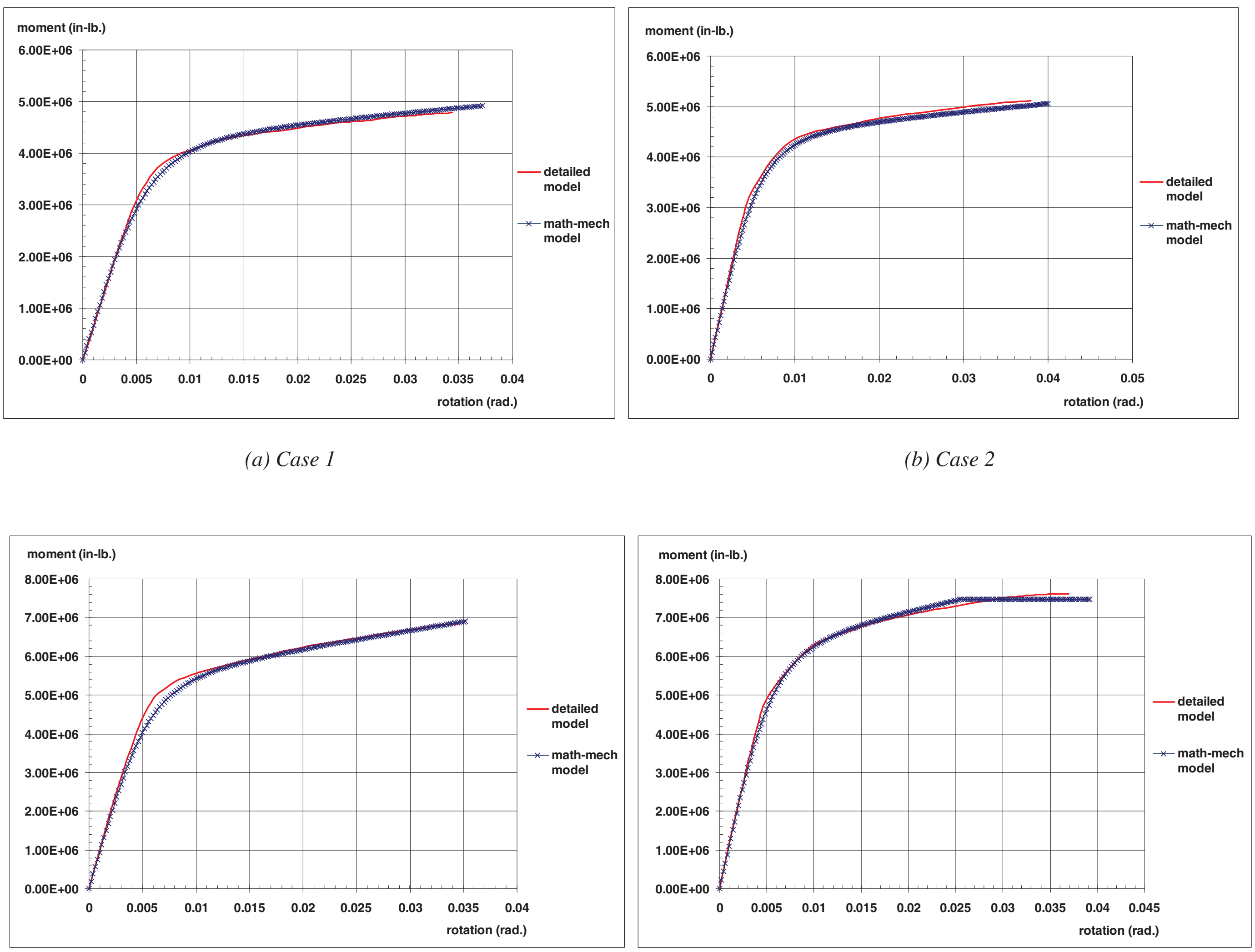

(a) Case 1 (b) Case 2

(c) Case 3 (d) Case 4

Fig. 8. Comparisons of the curves from mathematical-mechanical model with simulation results from detailed model.

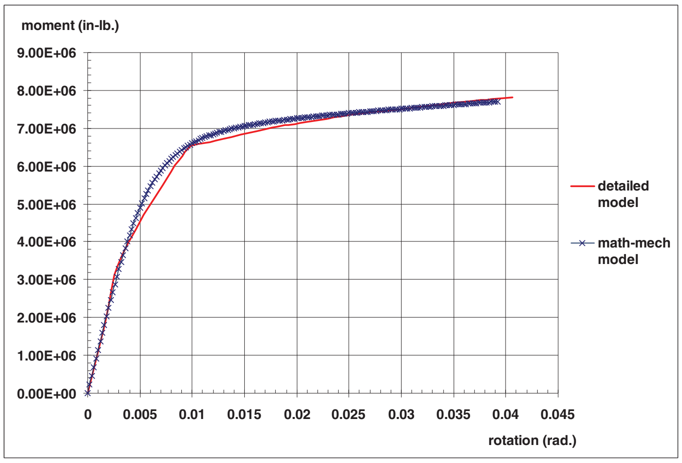

(e) Case 5

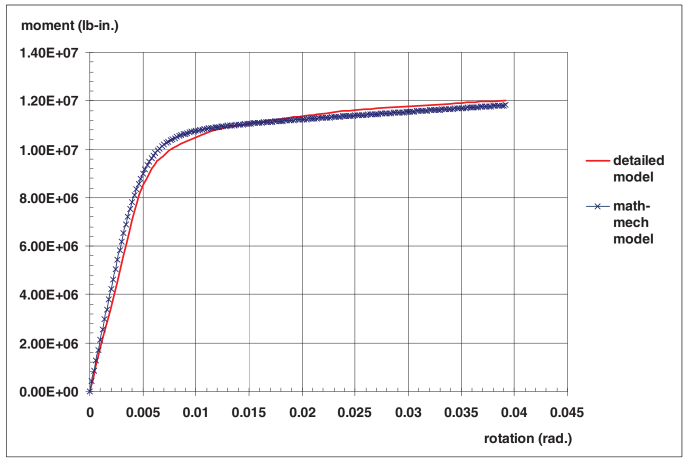

(f) Case 6

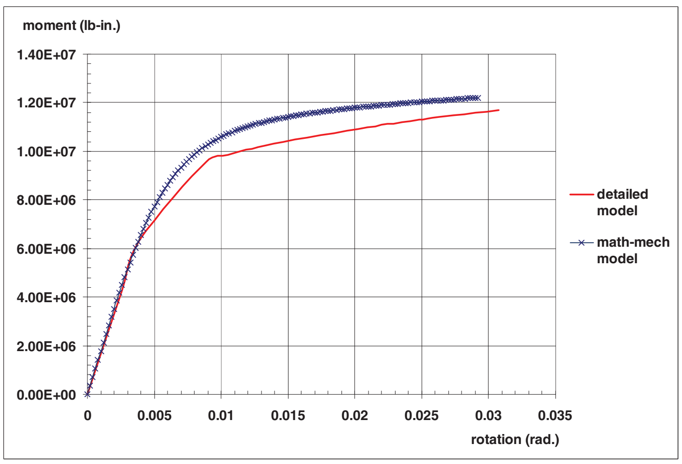

(g) Case 7

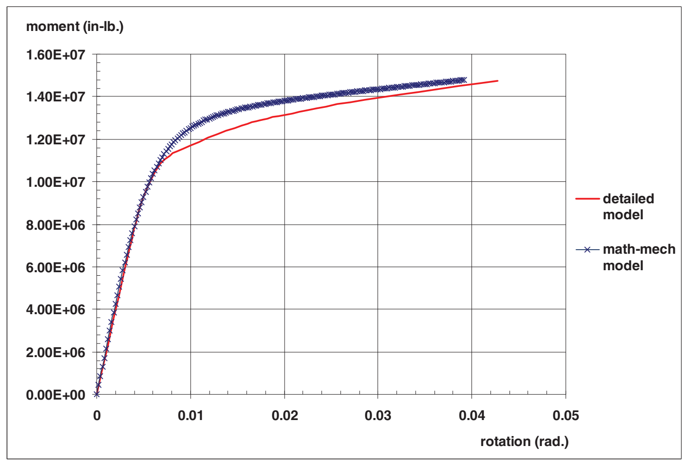

(h) Case 8

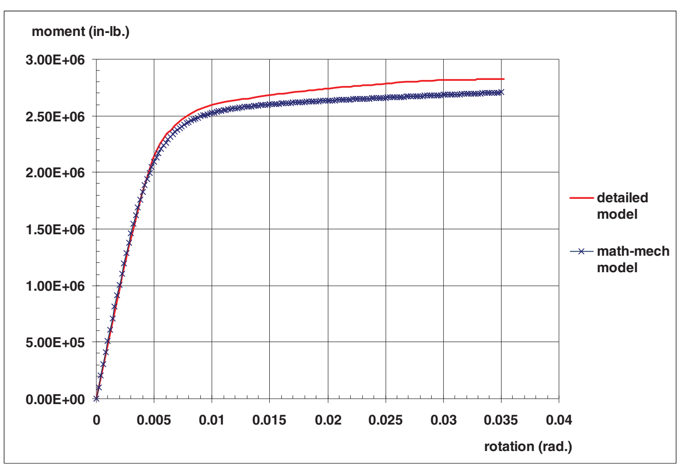

(i) Case 9

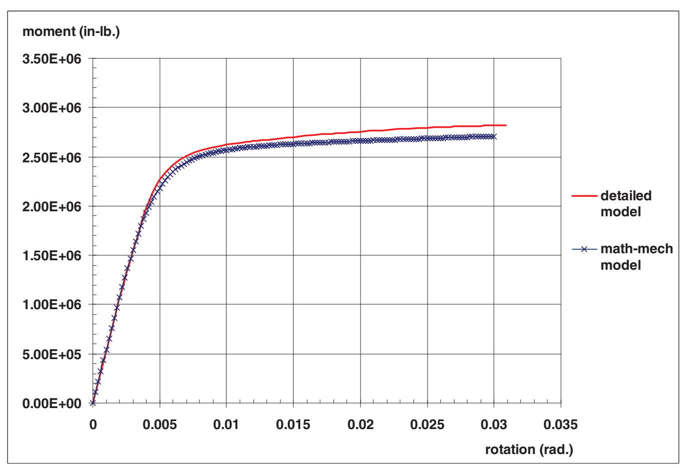

(j) Case 10

Fig. 8. Comparisons of the curves from mathematical-mechanical model with simulation results from detailed model (continued).

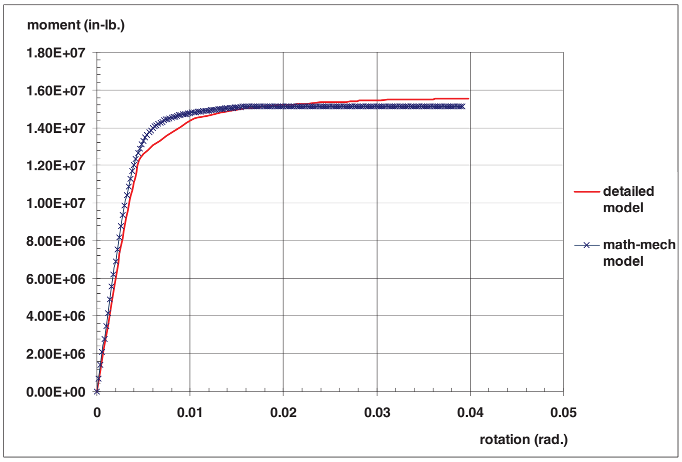

(k) Case 11

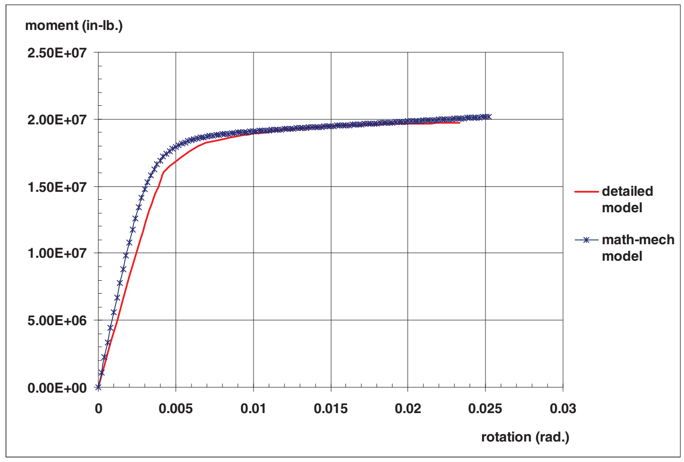

(l) Case 12

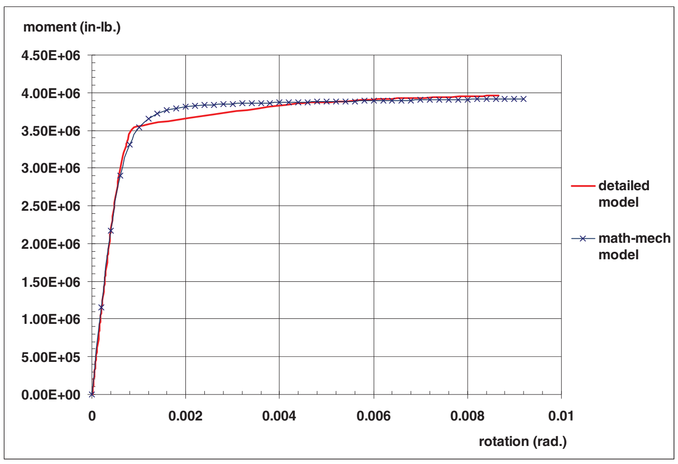

(m) Case 13

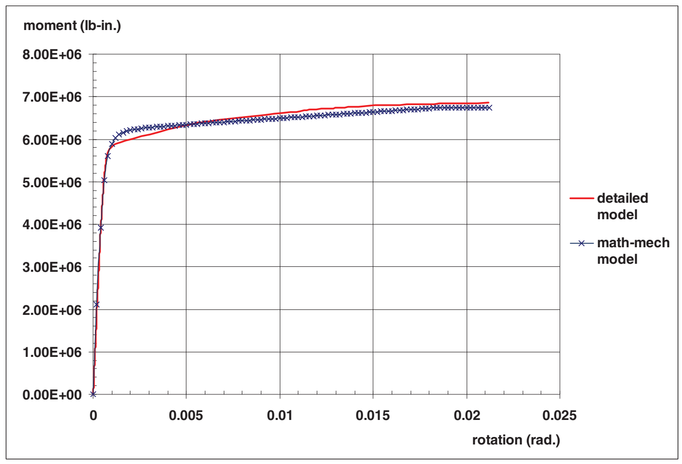

(n) Case 14

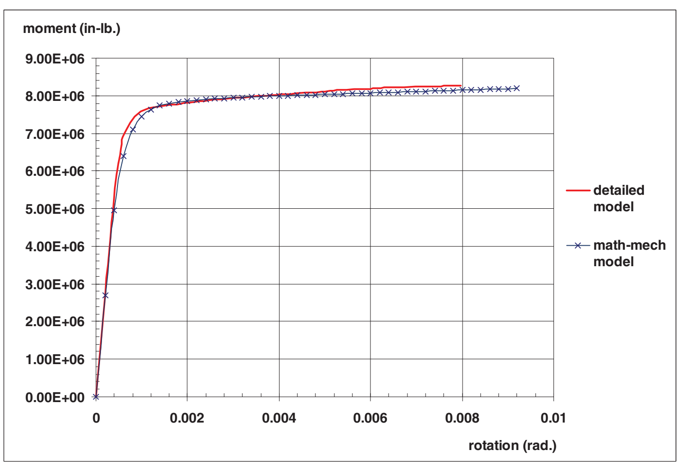

(o) Case 15

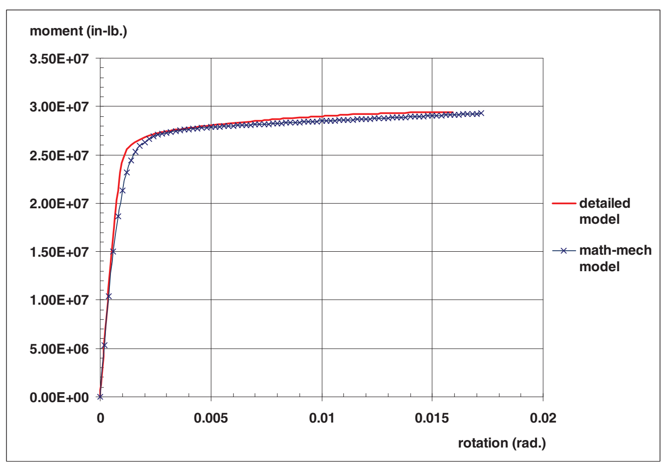

(p) Case 16

Fig. 8. Comparisons of the curves from mathematical-mechanical model with simulation results from detailed model (continued).

between the mathematical-mechanical models and the FEM simulations are less than 10 percent. These differences are probably due to the simplification of the detailed connection assembly. The $M - \theta$ curves produced in the mathematical-mechanical model were determined by mechanically defining the critical yield and ultimate points in terms of spring component behaviors and then mathematically connecting the points. In the FEM simulations, on the other hand, the $M - \theta$ curves were obtained by means of calculations of forces and deformations on a mesh of densely discrete elements, so that they can reflect the precise propagation of yielding and ultimate conditions in the girders and panel zones. Although the transition between pre-yield to post-yield behavior in the mathematical-mechanical model is based on two points and a shape factor, the derived curves compared well with the results from detailed simulations.

CONCLUSIONS

This study presents a comprehensive mathematical-mechanical modeling approach to define the resistance function of the welded unreinforced flange-bolted web (WUF-B) connection. The approach utilized a mathematical model for nonlinear characteristics, and a component method for coupling of individual components. A connection in a steel frame is a configuration of components that contains different geometries, shapes, and material properties. The same connection type may show diverse behavior, depending on the assembled components. Connection yielding will flow through the weakest component and spread to adjacent areas. Based on the hypothesis, this study considered the combined behaviors of individual components, since each of the assembled elements affects the combined behavior. In

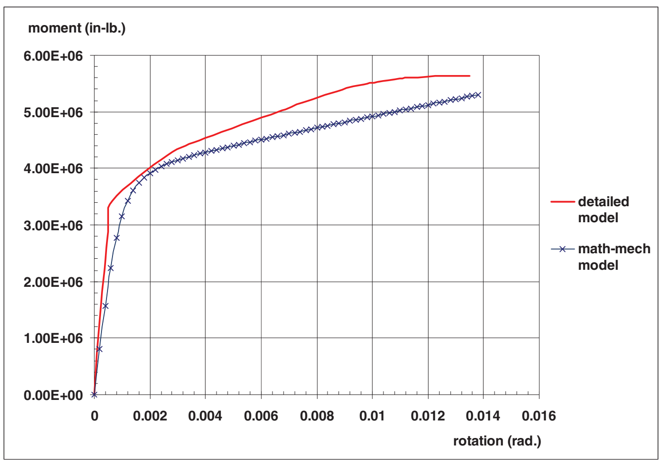

(q) Case 17

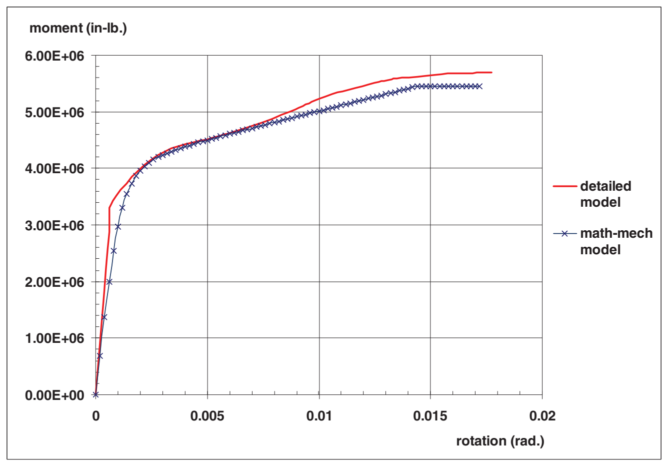

(r) Case 18

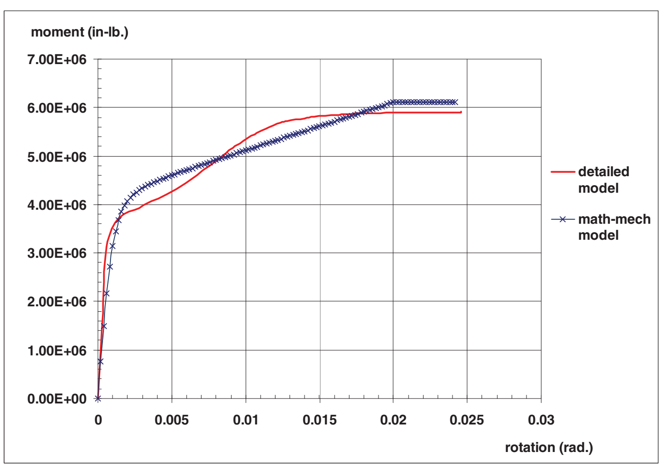

(s) Case 19

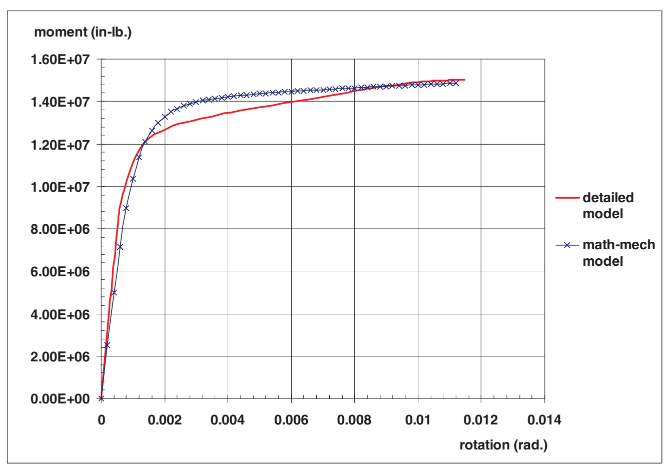

(t) Case 20

Fig. 8. Comparisons of the curves from mathematical-mechanical model with simulation results from detailed model (continued).

order to evaluate the representation approaches proposed in this study, various possible cases were selected that show the yield flows in different directions. Then, by tracing the responses, appropriate equations were collected, modified, and newly developed for each component property. The WUF-B connections were reclassified according to strength comparison of panel zones and girder regions. Comparisons of the $M - \theta$ curves showed that the mathematical-mechanical models developed in this study are able to accurately predict the resistance functions for the selected connections. Since a steel building generally includes a large number of connections, this mathematical-mechanical method is expected to reduce computational effort while providing acceptable levels of accuracy in the frame analysis.

ACKNOWLEDGMENT

This study was conducted with the generous support from the U.S. Army Engineer Research and Development Center.

REFERENCES

AISC (2005), *Steel Construction Manual,* 13th Edition, American Institute of Steel Construction, Chicago, IL.

Attiogbe, E. and Morris, G. (1991), "Moment-Rotation Functions for Steel Connections," *Journal of Structural Engineering*, ASCE, Vol. 117, pp. 1703–1717.

Carter, C.J. (2003), *AISC Steel Design Guide 13, Stiffening of Wide-Flange Columns at Moment Connections: Wind and Seismic Applications*, American Institute of Steel Construction, Chicago, IL.

Dassault Systems (2008), *ABAQUS User Manual*, Version 6.7-EF, ABAQUS.

Engelhardt, M.D. and Husain, A.S. (1992), "Cyclic Tests on Large Scale Steel Moment Connections," Report No. PMFSEL-92-2, Phil M. Ferguson Structural Engineering Laboratory, Department of Civil Engineering, Universtiy of Texas at Austin.

Engelhardt, M.D. and Sabol, T.A. (1994), "Testing of Welded Steel Moment Connections in Response to the Northridge Earthquake," Progress Report to the AISC Advisory Subcommittee on Special Moment Resisting Frame Research.

European Prestandard (1997), "Eurocode 3—Part 1.1 Revised Annex J: Joint in Building Frames," European Committee for Standardization (CEN), Brussels, Belgium.

Faella, C., Piluso, V. and Rizzano, G. (2000), *Structural Steel Semi-rigid Connections—Theory, Design and Software*, CRC Press.

FEMA (2000), "State of the Art Report on Systems Performance of Steel Moment Frames Subjected to Earthquake Ground Shaking," FEMA 355C, Prepared by the SAC Joint Venture for the Federal Emergency Management Agency, Washington, DC.

Ivany, M. and Baniotopoulos, C.C. (2000), "Semi-Rigid Connections in Structural Steelwork," Springer Wien New York (SPIN).

Kishi, N. and Chen, W.F. (1986), "Database of Steel Beam-to-Column Connections," Structural Engineering Report No. CE-STR-86-26, Vol. 2, School of Civil Engineering, Purdue University, West Lafayette, IN.

Kishi, N. (1994), "Advanced Analysis of Steel Frames," ed. Chen, W.F. and Toma, S., CRC Press.

Krauthammer, T., Lim, J., Choi, H. and Elfahal, M. (2004), *Evaluation of Computational Approaches for Progressive Collapse and Integrated Munitions Effects Assessment*, PTC-TR-002-2004, the Protective Technology Center, Pennsylvania State University, University Park, PA.

Krawinkler, H. (1971), "Inelastic Behavior of Steel Beam-to-Column Subassemblages," Ph.D. dissertation, University of California, Berkeley, CA.

Lim, J.H. and Krauthammer, T. (2006), "Progressive Collapse Analyses of 2D Steel-Framed Structures with Different Connection Models," *Engineering Journal*, AISC, Vol. 43, No. 3, pp. 201–215.

Nethercot, D.A., (1985), "Utilizations of Experimentally Obtained Connection Data in Assessing the Performance of Steel Frames," *Connection Flexibility and Steel Frames*, ed. Chen, W.F., American Society of Civil Engineers, Reston, VA.

Richard, R.M. and Abbott, B.J. (1975), "Versatile Elastic Plastic Stress-Strain Formula," *Journal of Engineering Mechanics*, ASCE, Vol. 101, No. 4, pp. 511–515.

Rassati, G.A., Leon, R.T. and Noe, S. (2004), "Component Modeling of Partially Restrained Composite Joints under Cyclic and Dynamic Loading," *Journal of Structural Engineering,* ASCE, Vol. 130, No. 2, pp. 343–351.

Simoes da Silva, L., Santiago, A. and Real, P.V. (2002), "Post-Limit Stiffness and Ductility of End-Plate Beam to Column Steel Joints," *Computers and Structures*, Vol. 80, No. 5–6, pp. 515–531.

Tamboli, A.R. (1999), *Handbook of Structural Steel Connection Design and Details*, McGraw-Hill Companies, Inc., New York.

Tschemmernegg, F. (1988), "On the Nonlinear Behavior of Joints in Steel Frames," in *Connections in Steel Structures: Behavior, Strength and Design*, ed. R. Bjorhovde et. al., Elsevier Applied Science, London, United Kingdom, pp. 158–165.

Yim, H.C. and Krauthammer, T. (2009), "Load-Impulse Characterization for Steel Connection," *Interntional Journal of Impact Engineering*, Vol. 36, No. 5, pp. 737–745.

Uang, C.M. and Bondad, D. (1996), "Static Cyclic Testing of Pre-Northridge and Haunch Repaired Steel Moment Connections," Report No. SSRP-96/02, Division of Structural Engineering, University of California, San Diego.